



ELSEVIER

Journal of Molecular Catalysis A: Chemical 114 (1996) 221–228

JOURNAL OF  
MOLECULAR  
CATALYSIS  
A: CHEMICAL

# Investigation of the manganese-substituted $\alpha$ -Keggin-heteropolyanion $K_6SiW_{11}O_{39}Mn(H_2O)$ by cyclic voltammetry and its application as oxidation catalyst

Masahiro Sadakane, Eberhard Steckhan \*

*Institut für Organische Chemie und Biochemie der Universität Bonn, Gerhard-Domagk-Straße 1, D-53121 Bonn, Germany*

## Abstract

The behavior of a manganese substituted  $\alpha$ -Keggin silicon tungstoheteropolyanion ( $K_6SiW_{11}O_{39}Mn(II)(H_2O)$ ) under electrochemical oxidation conditions was investigated by means of cyclic voltammetry in phosphate buffer. Substitution of the water ligand by counter anions (L:  $H_2PO_4^-$  or  $HPO_4^{2-}$ ) leading to  $SiW_{11}O_{39}Mn(II)(L)$  was observed. Replacement of the counter anion by an aquo ligand was observed in cyclic voltammetry by continuous cycling. After oxidation of  $SiW_{11}O_{39}Mn(II)(L)$  to  $SiW_{11}O_{39}Mn(IV)(L)$ , this counter anion L was in turn substituted by  $OH^-$ . The thus formed complex  $SiW_{11}O_{39}Mn(IV)(OH)$  oxidizes different alcohols, the reactivity of which decreases as follows: 1-phenyl-ethanol, benzylalcohol > *iso*-propanol > ethanol.

**Keywords:** Keggin ions; Ligand exchange; Manganese; Cyclic voltammetry; Alcohol oxidation

## 1. Introduction

Homogeneous catalytic oxidations have been one of the most interesting areas of chemical research. Numerous metalloporphyrin-based systems including iron, manganese, cobalt, chromium and ruthenium have been described [1]. Recently, considerable attention has been directed towards metal substituted  $\alpha$ -Keggin heteropolyanions as analogues of metalloporphyrins [2].

From  $\alpha$ -Keggin heteropolyanions ( $AB_{12}O_{40}$ ), so-called 'lacunary heteropolyanions' ( $AB_{11}O_{39}$ ) are derived by removing one  $BO_6$  unit. Many transition metals (Co, Cr, Fe, Mn, Ru etc.) can

fill this hole, giving rise to metal substituted  $\alpha$ -Keggin heteropolyanions such as  $PW_{11}O_{39}Co(H_2O)$ . Similar to metalloporphyrins, metal substituted  $\alpha$ -Keggin heteropolyanions can work as oxygen carriers. These transition metals  $M^{n+}$  accept oxygen from different oxygen donors (e.g. iodosylarenes, peroxides, etc.) and the thus formed oxometal species  $M^{n+2}=O$  are able to oxidize various organic substrates like hydrocarbons, alcohols and olefins [2]. The heteropolyanion ligands are robust under strongly oxidative conditions and thus have an important advantage over metalloporphyrin systems, which decompose under these conditions.

The electrochemical properties of the  $PW_{11}O_{39}Ru$  [3,4],  $PW_{11}O_{39}Cr$  [5],  $SiW_{11}O_{39}Fe$  [6–8],  $SiW_{11}O_{39}Re$  and  $PW_{11}O_{39}Re$  [9] have

\* Corresponding author.

been reported. The transition metal incorporated in the heteropolyanion resides in an octahedral environment with one coordination site occupied by a labile water molecule. On electrochemical oxidation in aqueous media this water ligand works as oxygen source. The aquo transition metal complex  $M(\text{III})(\text{H}_2\text{O})$  ( $M = \text{Ru}, \text{Cr}$  and  $\text{Re}$ ) was oxidized to an oxo transition metal complex  $M(\text{V})=\text{O}$  by removing two protons. In our group, heteropolyanions have been used as electrochemical catalysts in a double-mediator system in combination with electrochemically generated  $\text{NaIO}_4$  [10]. In this work, we have focused our attention on manganese substituted  $\alpha$ -Keggin silicon tungstoheteropolyanion for the application as an electrochemically regenerable mono-mediator system. This complex ( $\text{SiW}_{11}\text{O}_{39}\text{Mn}(\text{II})$ ) can catalyze the oxidation of phenols, olefins and hydrocarbons in combination with some stoichiometric oxidants [2]. Recently, Pope and his co-workers have oxidized some Mn(II)-substituted polyoxotungstate  $\text{XW}_{11}\text{O}_{39}\text{Mn}(\text{II})(\text{H}_2\text{O})$  ( $X = \text{Si}, \text{P}, \text{B}$  and  $\text{Zn}$ ) chemically and electrochemically and characterized them by spectroscopy [11]. They proposed that in the electrooxidation the corresponding manganese complex is oxidized to the  $\text{Mn}(\text{IV})(\text{OH})$  complex rather than to  $\text{Mn}(\text{V})(=\text{O})$ . However, no detailed electrochemical studies of this complex have appeared. In this paper, we want to present the electrooxidative behavior of  $\text{K}_6\text{SiW}_{11}\text{O}_{39}\text{Mn}(\text{II})(\text{H}_2\text{O})$  as examined by means of cyclic voltammetry and application as oxidation catalyst.

## 2. Experimental

### 2.1. Material

The potassium salts of the lacunary heteropolyanion  $\text{K}_8\text{SiW}_{11}\text{O}_{39}\cdot 13\text{H}_2\text{O}$  [12] and the manganese substituted Keggin heteropolyanion  $\text{K}_6\text{SiW}_{11}\text{O}_{39}\text{Mn}(\text{II})(\text{H}_2\text{O})\cdot 6\text{H}_2\text{O}$  [13] were prepared as the  $\alpha$ -isomer according to the procedure described previously. The water content of

the isolated salts was calculated from thermogravimetric measurements based on the total loss in weight until 350°C. Each solution was prepared from  $\text{KH}_2\text{PO}_4$  (Ferak Berlin, Analytic Grade),  $\text{KOH}$  (Riedel–de Haén, reagent grade), 85%  $\text{H}_3\text{PO}_4$  (Riedel–de Haén, reagent grade) and water that had been purified by passage through a purification train. All alcohols used in the kinetics study, were of analytical grade and used without further purification.

### 2.2. Equipment and procedures

Electrochemical measurements were conducted with conventional commercially available instruments using two- or three-compartment cells with a BAS100B/W system (Bioanalytical Systems, West Lafayette, Indiana). A glassy carbon working electrode, a platinum wire counter electrode and a  $\text{Ag}/\text{AgCl}$  reference electrode (3 M  $\text{KCl}$ , Cypress Systems, Inc., Lawrence, Kansas) were used. The glassy carbon working electrode (diameter 3 mm) was polished with silicon carbide (1000 mesh), washed with bi-distilled water before use without previous sonication [6]. The experiments were conducted at ambient temperature.  $E_{1/2}$  values were calculated from cyclic voltammetry as the average of the cathodic and anodic peak potentials for the oxidative and reductive waves. UV–vis spectra were recorded at 25°C by using a Cary 1 UV–vis spectrometer (Varian) with a 1 cm quartz cells. Thermogravimetric analyses were obtained with STA/QMS-system 409/429-403 (Netzsch-Gerätebau, Selb).

## 3. Results and discussion

### 3.1. Cyclic voltammetry

Fig. 1(a) shows a cyclic voltammogram of a 1 mM solution of the ‘lacunary heteropolyanion’  $\text{K}_8\text{SiW}_{11}\text{O}_{39}$  in 0.5 M  $\text{KH}_2\text{PO}_4$  solution (pH 4.2). The two large reversible peaks can be attributed to the two two-electron reduction steps

of the lacunary heteropolyanion  $K_8SiW_{11}O_{39}$ . The two small reduction waves are supposed to be reduction peaks of  $SiW_{12}O_{40}^{4-}$  incorporated as impurities. A small peak that appears as a shoulder at  $-0.52$  V probably is an oxidation wave of the  $\beta$ -isomer which is generated during the reduction of the original  $\alpha$ -isomer at the potential of the second wave [6]. Therefore, this anodic wave attributed to the  $\beta$ -isomer is absent at scan rates greater than  $500$   $mV s^{-1}$ . Fig. 1(b) shows a cyclic voltammogram of a  $1$  mM solution of  $K_6SiW_{11}O_{39}Mn(II)(H_2O)$  in  $0.5$  M  $KH_2PO_4$  (pH 4.2). The positions of the two two-electron reduction waves for the lacunary anion moved slightly as compared with the manganese free system, and the fact that the magnitudes of the pair of cathodic peaks for the Mn(II) derivatives were almost identical with those of the parent anions shows that the Mn(II) center is not reducible to Mn(I) within the potential range examined in Fig. 1. Two new redox pairs at  $0.59$  V (anodic) and  $0.47$  V

(cathodic), respectively at  $1.14$  V (anodic) and  $1.00$  V (cathodic) appeared. The second oxidation wave was superimposed on the anodic background current. In the pH 6.0 solution ( $0.5$  M  $KH_2PO_4 + 0.5$  M KOH, Fig. 1(c)), the reversible redox pair at  $0.60$  V (anodic) and  $0.48$  V (cathodic) was retained, while the oxidation peak for the second redox pair was almost indistinguishable from the background current. The respective reduction peak was observed at  $0.93$  V. As shown in Fig. 2, with continuous scanning of the potential region from  $0$  to  $1.3$  V, the first oxidative peak shifted to a more negative potential, and the second oxidation peak developed with increasing number of scans. Additionally, all peak currents increased. Fig. 3 shows the change of the peak potential,  $E_{1/2}$ , and the peak current of the first redox pair with the number of scans. With continuous cycling, all peaks finally reach a stable value (consolidated peaks). The appearance of the voltammograms at the first scan varied slightly depending

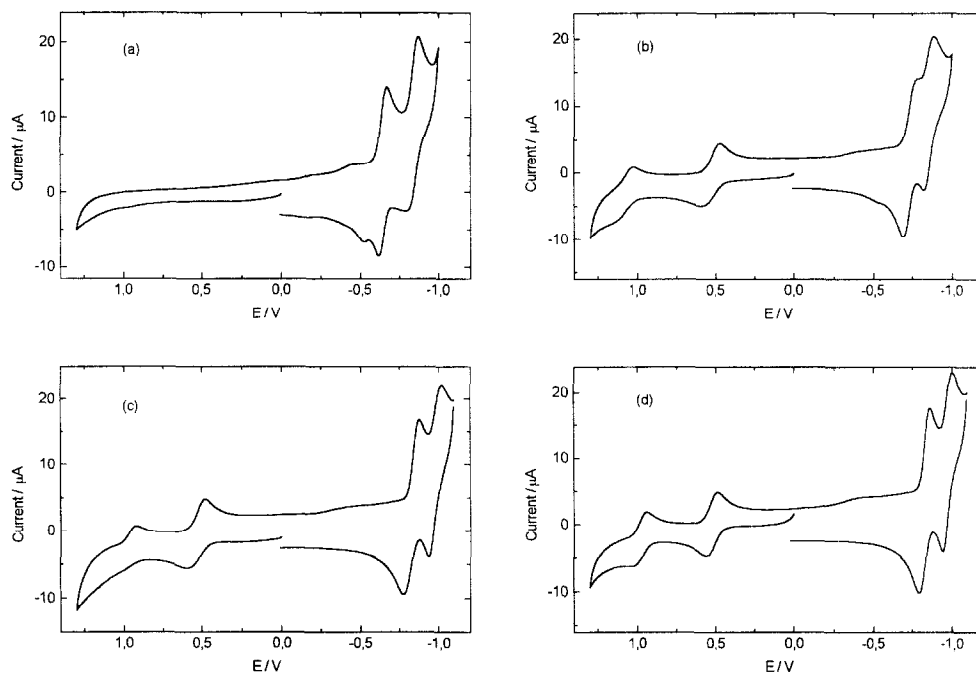


Fig. 1. Cyclic voltammograms at a glassy carbon electrode of (a) a  $1$  mM solution of the 'lacunary heteropolyanion' in phosphate buffer (pH 4.2); (b) the Mn(II) substituted derivative in phosphate buffer (pH 4.2); (c) the same as (b) however in phosphate buffer of pH 6.0; (d) consolidated peaks after continuous scanning of the solution used in (c). Supporting electrolyte:  $0.5$  M phosphate solution. Scan rate =  $20$   $mV s^{-1}$ . The initial potential was  $0$  V and the initial scan direction was towards more positive potential.

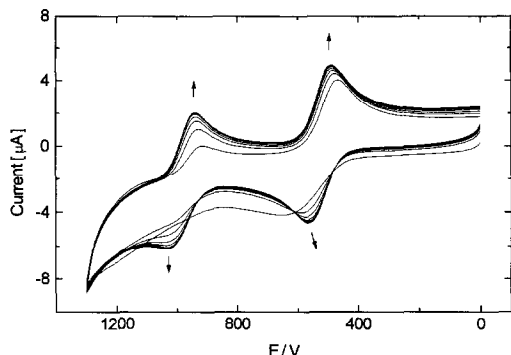


Fig. 2. Continuous cyclic voltammograms at a glassy carbon electrode of a 1 mM solution of  $\text{SiW}_{11}\text{O}_{39}\text{Mn}$  in pH 6.0 phosphate buffer. Supporting electrolyte: 0.5 M phosphate solution. Scan rate =  $20 \text{ mV s}^{-1}$ . The initial potential was 0 V and the initial scan direction was towards more positive potential. The arrows indicate the direction of peak changes during continuous scanning.

on the electrode surface condition, but during continuous cycling of the potential region between 0 and 1.3 V the waves always ap-

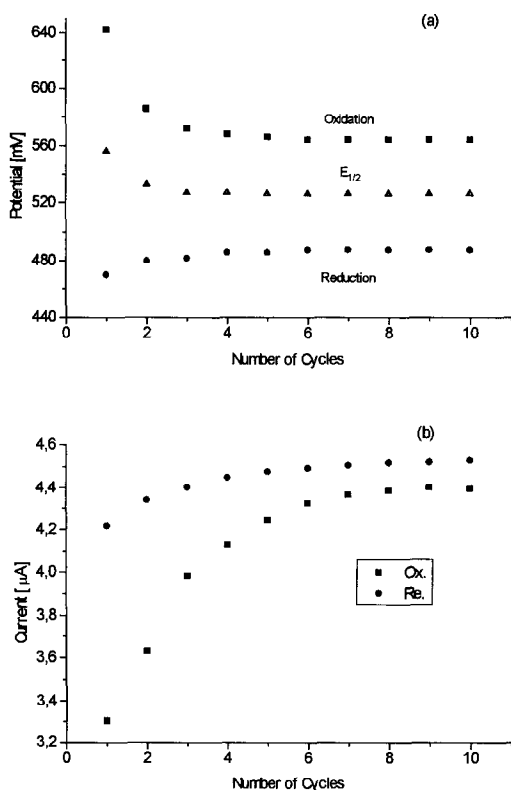


Fig. 3. Change of (a) anodic and cathodic peak potential and  $E_{1/2}$  and (b) the anodic and cathodic peak currents of the  $\text{Mn}(\text{II}/\text{III})$  pair during continuous scanning between 0 V and 1.3 V.

proached the same consolidated peaks. This tendency was also observed at pH 4.2 (0.5 M  $\text{KH}_2\text{PO}_4$  solution). The two redox waves in the positive potential area were growing and reached the consolidated peaks. All peak currents were linearly depending on the square root of the voltage scan rate ( $1\text{--}144 \text{ mV s}^{-1}$ ) indicating that all electrode processes are diffusion controlled. Each of these two consolidated reversible redox pairs corresponds to a single electron transfer. This is suggested by the peak currents of these oxidation peaks being roughly equal to half the value of those of the 2-electron-reduction peaks in Fig. 1(d) and was also confirmed by the charge consumption in exhaustive electrolysis (vide infra). Therefore, the redox couples could be attributed to the redox pairs  $\text{Mn}^{\text{II}/\text{III}}$  and  $\text{Mn}^{\text{III}/\text{IV}}$ , respectively.

The shape-change of the voltammogram by continuous cycling during cyclic voltammetry was also observed in other solutions like 0.5 M  $\text{KOAc}$ , 0.5 M  $\text{KCl}$  and 0.1 M  $\text{KClO}_4$  in the pH range in which the heteropolyanion is stable [13].

### 3.2. Effect of pH and ion strength

Because the peaks of the first scan depended on the electrode pretreatment, the attention was first focused on the consolidated peaks. Within the pH ranges in which the compounds were stable [13], the effect of the pH upon the redox potentials of the stable peaks is summarized. The peak separations were typically 70–100 mV. Fig. 4(a) shows the dependence of  $E_{1/2}$  on the pH value with constant potassium concentration for the two anodic waves. The  $E_{1/2}$  of  $\text{Mn}^{\text{III}/\text{IV}}$  showed a clear linear dependence on the pH with a slope of 57 mV per pH value. This means that one proton is involved in the redox step. The consolidated redox couple  $\text{Mn}^{\text{II}/\text{III}}$ , however, shows no pH dependence but depends on the concentration of the potassium cation. As shown in Fig. 4(b), the  $E_{1/2}$  of  $\text{Mn}^{\text{II}/\text{III}}$  changed ca. 62 mV per  $-\log[\text{K}^+]$ . This suggests that the potassium cation is in-

volved in this redox step. The change of the  $E_{1/2}$  of  $\text{Mn}^{\text{III/IV}}$  with the concentration of potassium cations is negligible. This can be understood in analogy to the results reported by J.E. Toth and F.C. Anson [6] for the corresponding iron substituted heteropolyanion. They have reported a similar dependence of the peak potential on the cation concentration of the electrolyte for the reduction of the iron substituted heteropolyanion  $\text{SiW}_{11}\text{O}_{39}\text{Fe(III)(H}_2\text{O)}^{5-}$ . This was rationalized by the formation of ion-pairs of the iron substituted heteropolyanion with the cation of the supporting electrolyte, facilitating the reduction of the very negative heteropolyanion.

### 3.3. Controlled potential electrolyses

To determine the number of transferred electrons more exactly, exhaustive controlled poten-

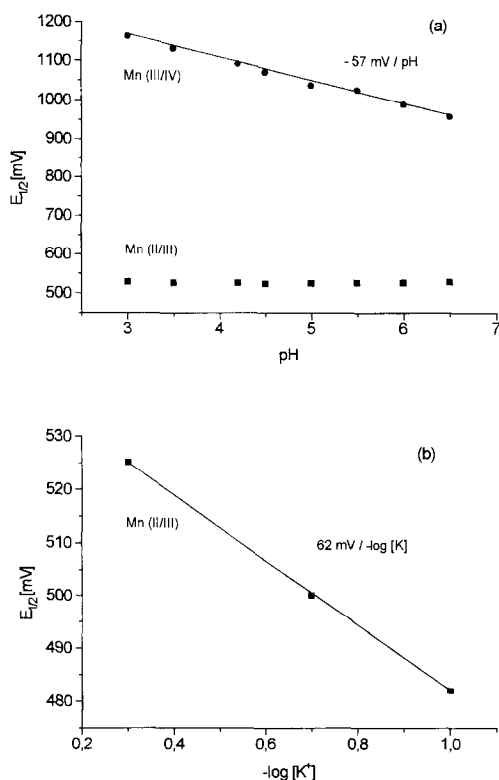


Fig. 4. (a) pH dependence of  $E_{1/2}$  for Mn(II/III) and Mn(III/IV) and (b) effect of potassium cation concentration of  $E_{1/2}$  of Mn(II/III).

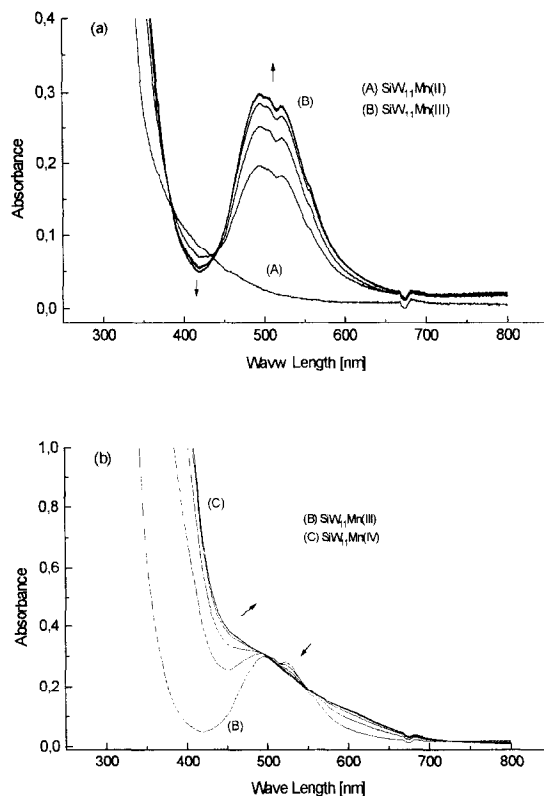
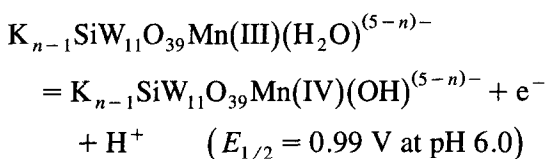
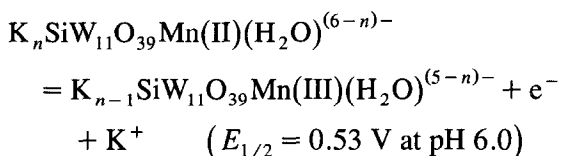


Fig. 5. UV-vis spectra of 1 mM of  $\text{SiW}_{11}\text{O}_{39}\text{Mn}$  by controlled potential electrolysis (a) at 0.85 V, and (b) at 1.25 V. The arrows indicate the direction of the absorbance changes during electrolysis.

tial electrolysis was carried out by using a carbon electrode, and the progress was monitored by UV-vis spectroscopy (Fig. 5). Correction for the background current was performed by using the BAS100B/W system. First, electrolysis was performed at 0.85 V until the UV-vis spectra did not change any more. A net charge of 0.92 F/mol was consumed until this point. The UV-vis spectrum (Fig. 5(a)) agreed with the previously reported spectrum of  $\text{SiW}_{11}\text{O}_{39}\text{Mn(III)}$  [13]. Then the potential was increased to 1.25 V, and the complex was electrolyzed at this potential until no further change of the UV-vis spectra (Fig. 5(b)) did occur. An additional net consumption of 0.99 F/mol was observed. Thus, at 0.85 V the Mn(III) complex was generated by a one-electron oxidation and at 1.25 V the Mn(IV)(OH) complex was formed by a second one-electron oxidation.

### 3.4. Electrochemical behavior of $\text{SiW}_{11}\text{O}_{39}\text{Mn}$ in the solution

The consolidated peaks in the cyclic voltammogram of  $\text{SiW}_{11}\text{O}_{39}\text{Mn(II)(H}_2\text{O)}^{6-}$  in the potential region between 0 V and 1.3 V versus Ag/AgCl can be explained quite easily by the following two reactions:



Both redox steps are quasi-reversible one electron processes. In the  $\text{Mn}^{\text{II/III}}$  step, the loss, respectively the uptake of a potassium cation forming an ion-pair is involved as indicated by the dependence of the potentials on the concentration of potassium cation. In the second step, for the  $\text{Mn}^{\text{III/IV}}$ -pair, one proton is involved as shown by the linear dependence of the peak potentials on the pH. Thus, the  $\text{Mn(IV)}$ -hydroxy species is obtained by anodic oxidation in aqueous buffer solution as has also been reported previously [11]. The  $\text{Mn(V)}$ -oxo species, however, could not be generated under these conditions.

For the shift of the peaks in the cyclic voltammogram during continuous scanning, several explanations are possible beforehand. For example, a change of the activity of the electrode surface must be taken into account. This can be excluded, however, because after the consolidated peaks have been obtained by continuous scanning, we stirred the solution for 15 min without touching the electrode, and received practically the same current–voltage curve as in the first scan. The activation of the electrode surface should, however, not have been altered to such an extent by this procedure. Secondly, the series of cyclic voltammograms during scan-

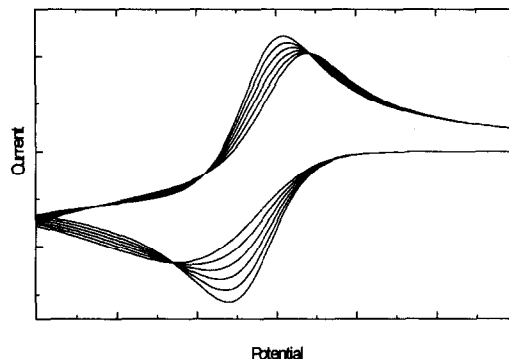
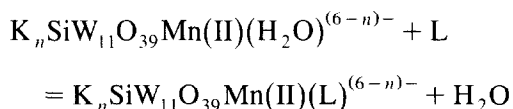


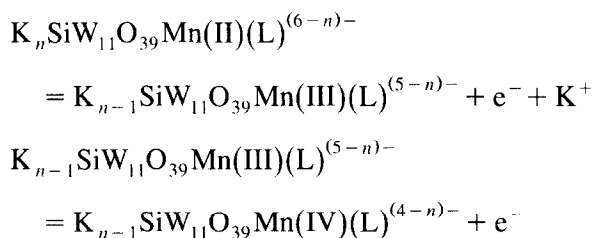
Fig. 6. Digital simulation: the initial complex A is converted to a different complex B in the course of the experiment. If the heterogeneous electron transfer rate is different for A and B, the conversion from A to B is accompanied by a shape change of the cyclic voltammogram, showing clear isosbestic points.  $A = B + e$ ,  $E_{1/2} = 0.525 \text{ V}$ ,  $k_s = 0.0001 \text{ (cm/s)}$ ,  $\alpha = 0.7$ ;  $C = D + e$ ,  $E_{1/2} = 0.525 \text{ V}$ ,  $k_s = 0.001 \text{ cm/s}$ ,  $\alpha = 0.7$   $D_A = D_B = D_C = D_D$ ,  $[A] + [B] = 1.0 \text{ mM}$ .

ning clearly show 'isosbestic' points (Fig. 2), which indicates that one compound is continuously transformed into one other compound during this process (Fig. 2). From the shape of the voltammograms, it can be deduced that for the initial redox system, the heterogeneous electron transfer rate is considerably slower than for the redox system which is formed during continuous cycling, while the redox potentials are practically the same for both systems. (Digital simulation of this process using the DigSim® 2.0 (Bioanalytic Systems, West Lafayette, IN) proves our assumption (Fig. 6).) The initial heterogeneous electron transfer rate seems to depend on the electrode surface pretreatment, thus explaining the low reproducibility of the first scan. Because scanning of the potential region of only the first redox pair does not result in a potential shift, it can be concluded that the transformation occurs on the  $\text{Mn(IV)}$  stage. We also have to include into our argumentation the fact that freshly prepared solutions of  $\text{K}_6\text{SiW}_{11}\text{O}_{39}\text{Mn(II)(H}_2\text{O)}$  in 0.5 M  $\text{KH}_2\text{PO}_4$  (pH 4.2) show a larger similarity with the consolidated peaks than those which we obtained after letting the solution stay for some time. In addition, similar effects are observed in the presence of other anions of the supporting

electrolyte like perchlorate and acetate. Taking all this into account, we explain the potential shift during continuous scanning of the cyclic voltammogram by a ligand exchange reaction in the following way. At the beginning, the aquo ligand in the freshly prepared Mn(II) complex has been exchanged by the phosphate or other anions of the supporting electrolyte (L) in a slow reaction. The rate of this exchange reaction is influenced by the concentration of the  $\text{HPO}_4^{2-}$  ion in the phosphate buffer solution, which is different for pH 4.2 and pH 6.0. These solutions differ in the concentration of the phosphate anion,  $\text{H}_2\text{PO}_4^{1-}$  and  $\text{HPO}_4^{2-}$ . The higher concentration of  $\text{HPO}_4^{2-}$  in the solution of pH 6.0 caused a faster exchange of the aquo ligand (Fig. 1(b) and (c)) compared to the pH 4.2 solution. This can be seen in the cyclic voltammetry of a freshly prepared solution of the manganese heteropolyanion in pH 6.0 which already shows only the electrochemically slow redox pair in which the second anodic wave has shifted into the increase of the background current. Thus, the following exchange reaction occurred in solution (L:  $\text{H}_2\text{PO}_4^{1-}$  or  $\text{HPO}_4^{2-}$ ):

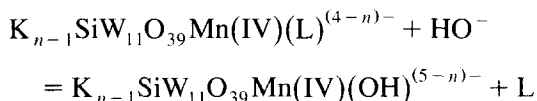


This redox system (maybe together with small amounts of the aquo complex) shows the initial cyclic voltammogram in which the oxidation peaks are shifted to positive values. The oxidation of  $\text{SiW}_{11}\text{O}_{39}\text{Mn(III)}(\text{L})^{(m-1)-}$  can almost not be distinguished from the background current of the electrolyte.



At the hard Mn(IV) oxidation state, the phosphate anion is easily replaced by the hard hydroxy

droxy group, thus transforming the redox system back to the hydroxy (aquo) complex:



In fact, if the cyclic voltammogram is recorded from an initial potential, where the Mn(IV)(OH) complex is produced at the electrode surface (1.25 V versus Ag/AgCl in pH 6.0 solution), the consolidated peaks were obtained immediately, instead of after multiple cycling. Therefore, by controlled potential electrolysis (at 1.25 V versus Ag/AgCl) the Mn(IV)(OH) complex is generated.

The retransformation of the manganese(IV) phosphate system into the manganese(IV) hydroxy complex at the second oxidation step makes the  $\text{SiW}_{11}\text{O}_{39}\text{Mn(IV)}(\text{OH})^{5-}$  system a promising candidate for the application as a mediator in indirect electrochemical oxidation processes.

### 3.5. Oxidative reactivity of $\text{SiW}_{11}\text{O}_{39}\text{Mn(IV)}(\text{OH})^{5-}$

The electrochemically generated Mn(IV)(OH) complex is slowly reduced to the Mn(III) complex at room temperature in the solution. Addition of alcohols to the solution accelerated this reduction. The Mn(IV)(OH) complex reacted with 1-phenyl-ethanol and produced the Mn(III) complex and acetophenone (detected by gas chromatography), indicating that the manganese-substituted silicon tungstoheteropolyanion can act as a catalyst for the electrochemical oxidation of alcohols.

Fig. 7 shows the UV-vis spectra of the reaction mixture in the course of the reaction of the Mn(IV)(OH) complex with *iso*-propanol. The spectral changes of the reaction show clean isosbestic points and the UV-vis spectrum of the complex after complete reduction is in fact virtually identical to that of  $\text{SiW}_{11}\text{O}_{39}\text{Mn(III)}$ . The kinetics of the oxidation of an alcohol by electrochemically generated Mn(IV)(OH) com-

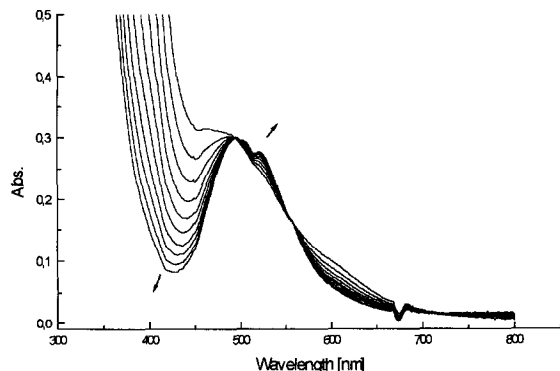


Fig. 7. UV-vis spectral changes for the reaction between  $\text{SiW}_{11}\text{O}_{39}\text{Mn(IV)(OH)}^{5-}$  (1 mM) and *iso*-propanol (0.5 M). Scan interval 5 min.

plex in phosphate solution has been studied by using *iso*-propanol. Under pseudo-first order condition ( $[\text{Mn}] \ll [\text{alcohol}]$ ), the appropriate logarithmic kinetic plots were linear ( $r > 0.9995$ ), establishing first order kinetics in the concentration of Mn. The observed rate ( $k_{\text{obs}}$ ) increased linearly with increasing concentration of *iso*-propanol (Fig. 8) and was independent of the pH of the solution. We compared the oxidation rate of some other alcohols in the pH 6.0 phosphate buffer at constant concentration of alcohols ( $[\text{alcohol}] = 0.1 \text{ M}$ ). The alcohols reacted with the  $\text{Mn(IV)OH}$  complex in the fol-

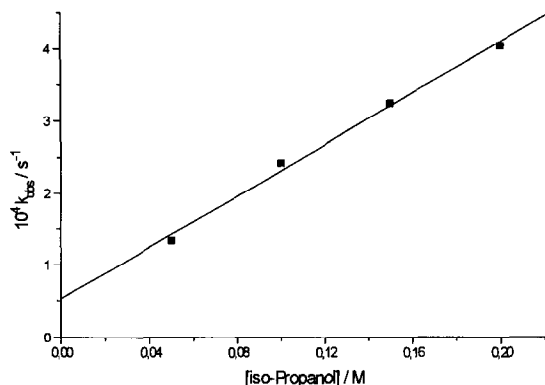


Fig. 8. Pseudo-first order rate constants ( $k_{\text{obs}}$ ) for the oxidation of *iso*-propanol by  $\text{SiW}_{11}\text{O}_{39}\text{Mn(IV)(OH)}^{5-}$  as a function of the concentration of *iso*-propanol. Supporting electrolyte: 0.5 M  $\text{KH}_2\text{PO}_4$  adjusted to pH 6.0 with 0.5 M KOH. Initial concentration of the heteropolyanion was 1.0 mM.

lowing order: 1-phenyl-ethanol ( $k_{\text{obs}} = 1.9 \times 10^{-3} \text{ s}^{-1}$ ), benzylalcohol ( $k_{\text{obs}} = 1.3 \times 10^{-3} \text{ s}^{-1}$ ) > *iso*-propanol ( $k_{\text{obs}} = 2.5 \times 10^{-4} \text{ s}^{-1}$ ) > ethanol ( $k_{\text{obs}} = 7.5 \times 10^{-5} \text{ s}^{-1}$ ).

#### 4. Conclusion

By means of cyclic voltammetry the electrochemical generation of  $\text{SiW}_{11}\text{O}_{39}\text{Mn(IV)(OH)}^{5-}$  by oxidation of  $\text{SiW}_{11}\text{O}_{39}\text{Mn(II)(H}_2\text{O)}^{6-}$  was demonstrated. The electrochemically generated  $\text{SiW}_{11}\text{O}_{39}\text{Mn(IV)(OH)}^{5-}$  is able to oxidize alcohols. A detailed mechanistic study and the preparative electrolysis are under investigation.

#### Acknowledgements

Financial support by the Volkswagen-Stiftung (AZ.: I/68384), the Fonds der Chemischen Industrie, and the BASF Aktien-Gesellschaft is gratefully acknowledged. The authors want to thank Mr. Eberhard Günther for the thermogravimetric analysis.

#### References

- [1] B. Meunier, Chem. Rev. 92 (1992) 1411.
- [2] C.L. Hill and C.M. Prosser-McCartha, Coord. Chem. Rev. 143 (1995) 407.
- [3] C. Rong and M.T. Pope, J. Am. Chem. Soc. 114 (1992) 2932.
- [4] J.C. Bart and F.C. Anson, J. Electroanal. Chem. 390 (1995) 11.
- [5] C. Rong and F.C. Anson, Inorg. Chem. 33 (1994) 1064.
- [6] J.E. Toth and F.C. Anson, J. Electroanal. Chem. 256 (1988) 361.
- [7] J.E. Toth, J.D. Melton, D. Cabelli, B.H.J. Bielski and F.C. Anson, Inorg. Chem. 29 (1990) 1952.
- [8] J.E. Toth and F.C. Anson, J. Am. Chem. Soc. 111 (1989) 2444.
- [9] F. Ortéga and M.T. Pope, Inorg. Chem. 23 (1984) 3292.
- [10] E. Steckhan and C. Kandzia, Synlett (1992) 139.
- [11] X.-Y. Zhang, M.T. Pope, M.R. Chance and G.B. Jameson, Polyhedron 14 (1995) 1381.
- [12] A. Tézé and G. Hervé, J. Inorg. Nucl. Chem. 39 (1977) 999.
- [13] C.M. Tourné, G.F. Tourné, S.A. Malik and T.J.R. Weakley, J. Inorg. Nucl. Chem. 32 (1970) 3875.